iScience, Volume *26*

Supplemental information

Suppression of *TREX1* deficiency-induced cellular senescence and interferonopathies by inhibition of DNA damage response

Hekang Du, Nanyang Xiao, Sitong Zhang, Xueyuan Zhou, Yangfan Zhang, Zengzeng Lu, Yuqian Fu, Miaohui Huang, Shan Xu, and Qi Chen

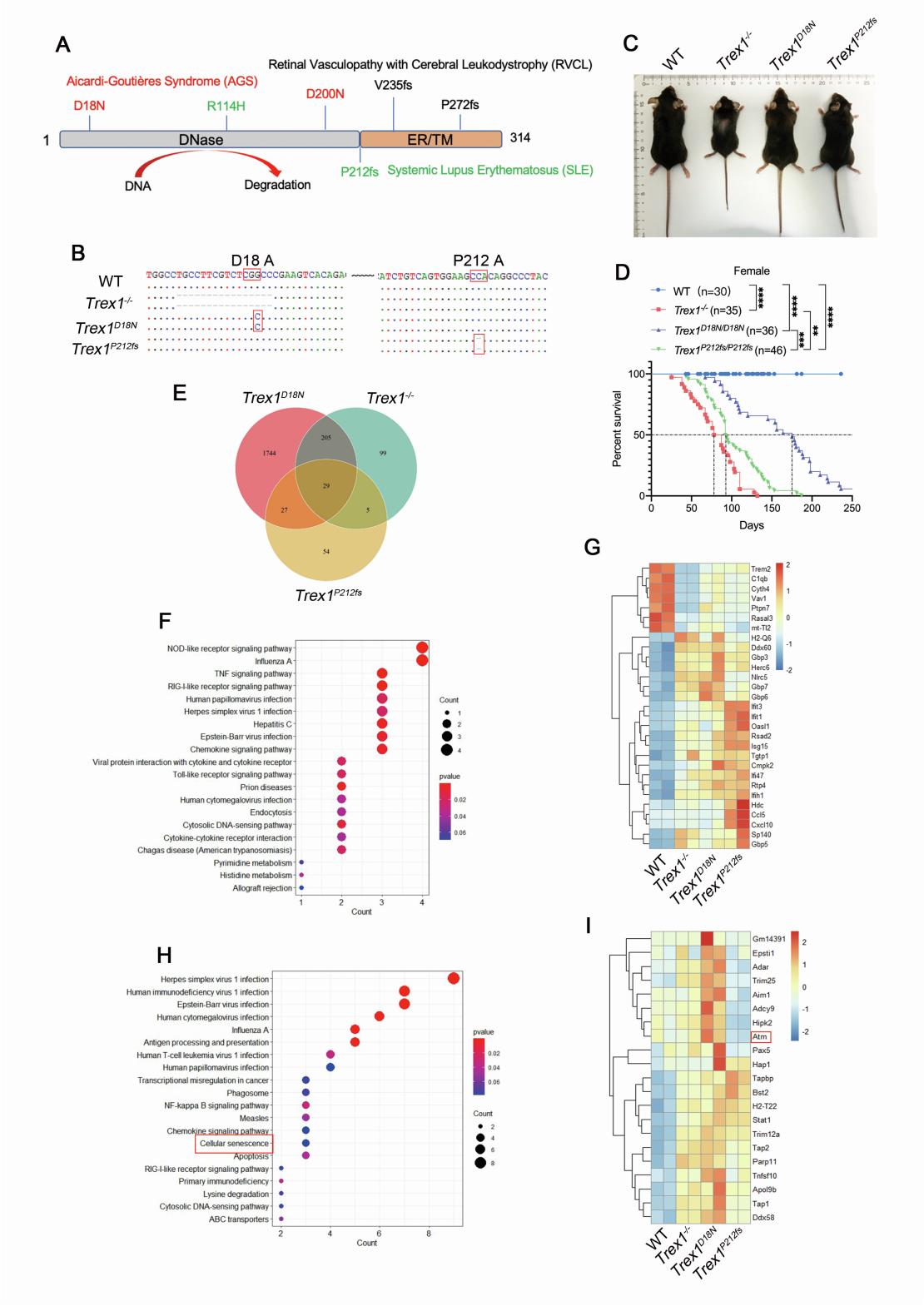

Figure S1. Differential gene expression analysis in *Trex1* gene-modified mouse models, Related to Figure 1.

(A) Diagram of common mutations in TREX1 associated with various autoimmune and inflammatory diseases. (B) Sequence of mutant loci in *Trex1*$^{-/-}$, *Trex1*$^{D18N/D18N}$, and *Trex1*$^{P212fs/P212fs}$ mice. (C) Representative 4–5-month-old WT, *Trex1*$^{-/-}$, *Trex1*$^{D18N/D18N}$, and *Trex1*$^{P212fs/P212fs}$ female mice. (D) Survival of WT, *Trex1*$^{-/-}$, *Trex1*$^{D18N/D18N}$, and *Trex1*$^{P212fs/P212fs}$

female mice. (E-I) Transcriptome analysis of primary MEFs from WT, *Trex1*$^{-/-}$, *Trex1*$^{D18N/D18N}$, and *Trex1*$^{P212fs/P212fs}$ E13.5 mice. (E) Gene expression in MEFs from the three gene-modified mouse models were compared with that of WT MEFs and the differential gene sets were plotted on a Venn diagram. (F) KEGG enrichment analysis of the differentially expressed genes common to all three *Trex1* gene-modified mouse models. (G) Heat map of differential gene expression. (H) 99 differentially expressed genes specific to *Trex1*$^{-/-}$ MEFs were analyzed by KEGG enrichment. (I) Heat map of gene expression in the pathway ($p < 0.01$), Data represent mean ±S.E.M. of at least 3 independent experiments. * $p < 0.05$; ** $p < 0.01$; *** $p < 0.001$, P values were calculated using one-way ANOVA versus WT with Dunnett's correction (D).

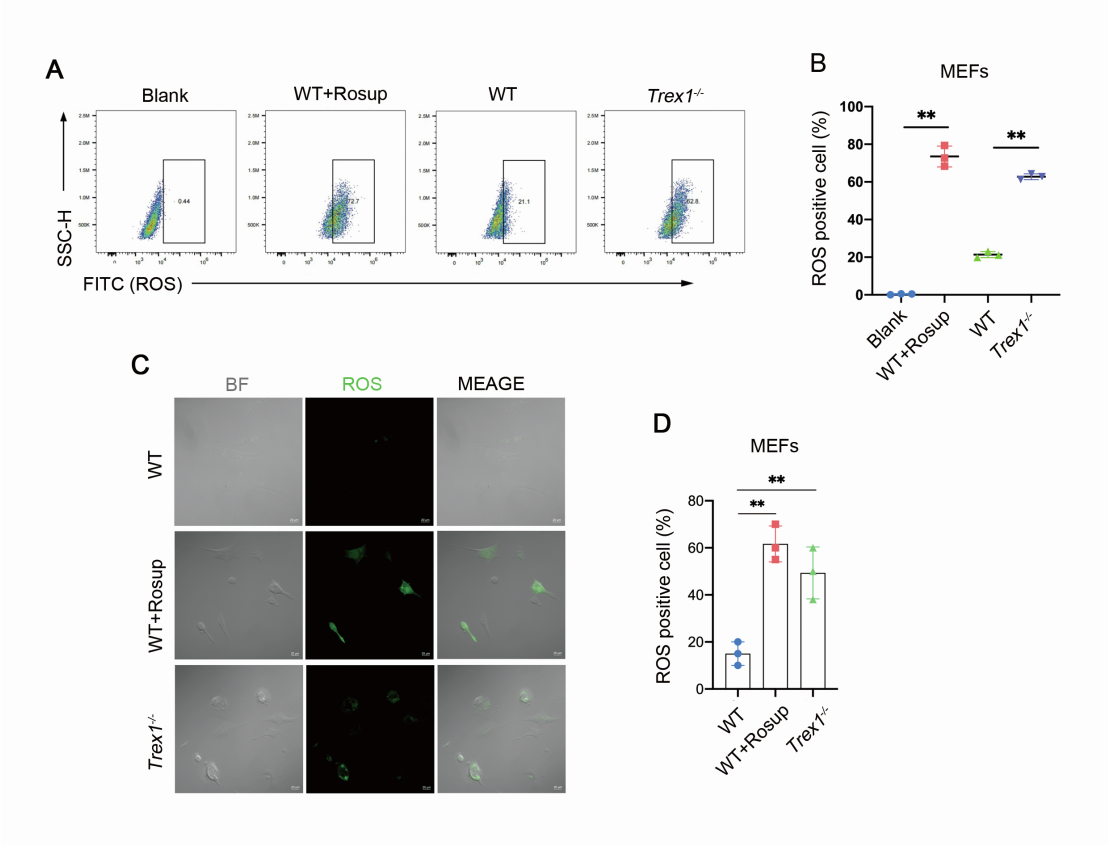

Figure S2. Dresence of high levels of ROS in *Trex1*$^{-/-}$ MEFs, Related to Figure 2.

MEFs were derived from E13.5 mouse embryos and cellular senescence was induced by serial passaging. The fluorescent probe DCFH-DA was incubated with passage 8 MEFs for 4 h; Rosup was used as a positive control. (A) ROS levels in *Trex1*$^{-/-}$ MEFs cells detected by flow cytometry. (B) Statistical results of flow cytometry (n=3 biological replicates). (C) ROS distribution in *Trex1*$^{-/-}$ MEFs observed by confocal microscopy. (D) Histograms indicate the percentages of positive cells by confocal microscopy (n=3 biological replicates). Data represent mean ± S.E.M. of at least 3 independent experiments. * $p < 0.05$; ** $p < 0.01$; *** $p < 0.001$, P values were calculated using one-way ANOVA versus WT with Dunnett's correction (B, D).

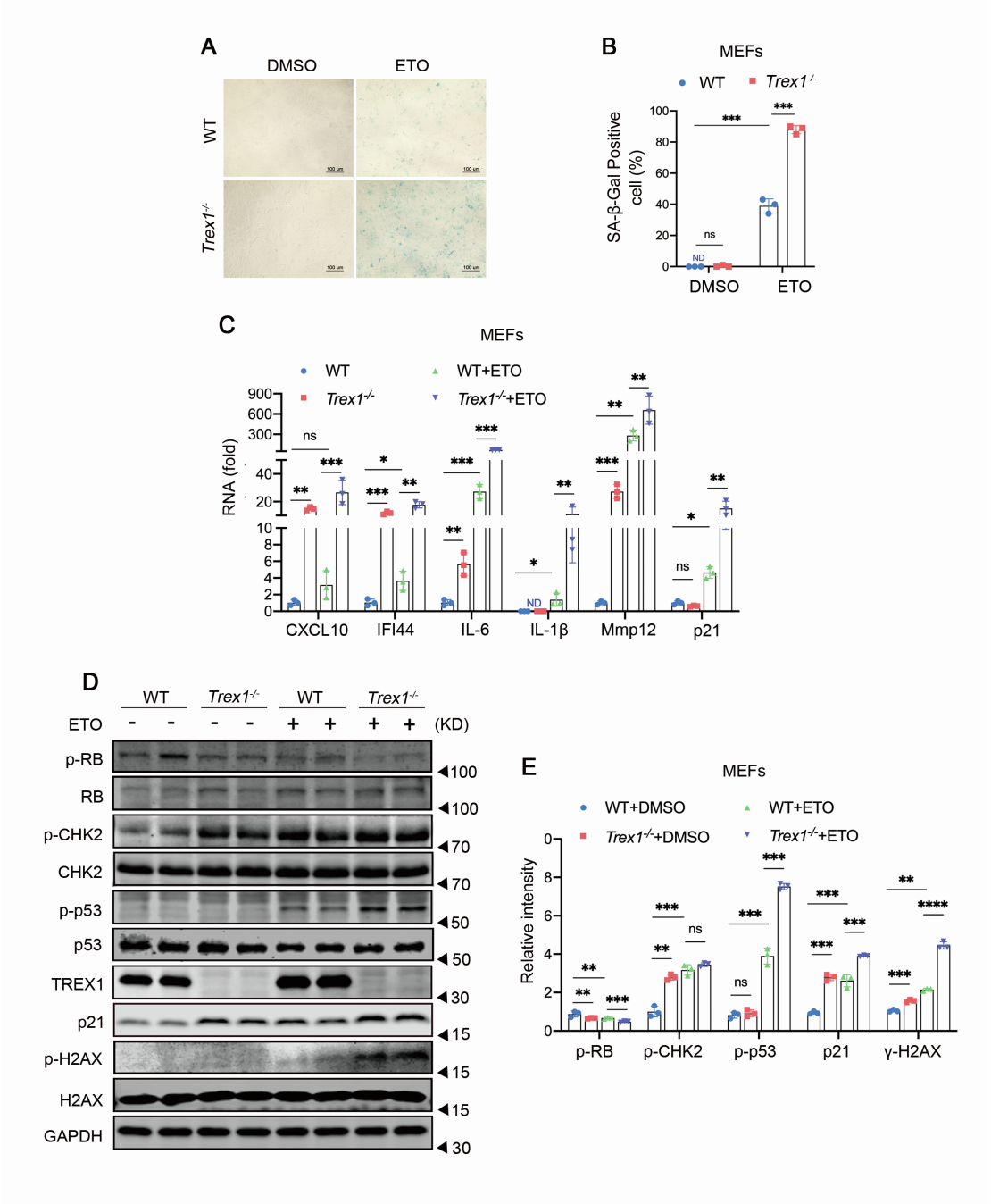

Figure S3. *Trex1* knockout amplifies etoposide-induced cellular senescence in MEFs, Related to Figure 3.

MEFs were derived from E13.5 mouse embryos. At 1 or 2 passage *Trex1*$^{-/-}$ MEFs were pre-treated with 10 μM etoposide (ETO), then changed to normal medium after 24 h and cultured for 5 days. (A) MEFs were subjected to SA-β-Gal analysis. (B) Histograms indicate the percentages of SA-β-Gal-positive cells (n=3 biological replicates). (C) Expression levels of SASP factors measured by RT-qPCR. (D) Expression of indicated proteins measured by immunoblotting. (E) Quantitative analysis of indicated proteins with GAPDH as control (n=3 biological replicates). Data represent mean ± S.E.M. of at least 3 independent experiments. * $p < 0.05$; ** $p < 0.01$; *** $p < 0.001$, P values calculated using two-way ANOVA with Bonferroni's correction (B, C, E). For gel source data, see Mendeley Data.

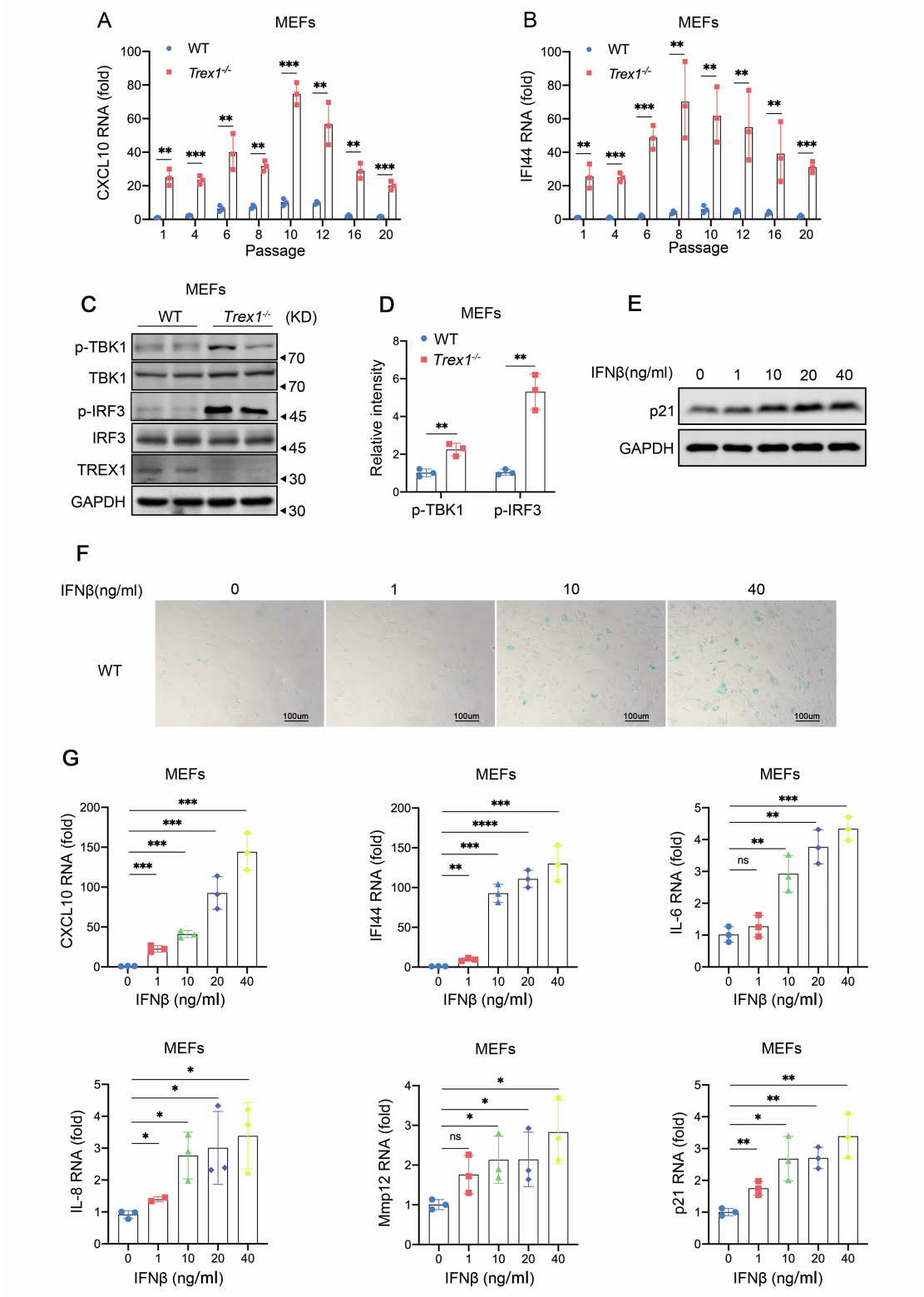

Figure S4. *Trex1* knockout activates the cGAS-STING pathway in MEFs, Related to Figure 4.

MEFs were derived from E13.5 mouse embryos and cellular senescence was induced by serial passaging. (A-B) RT-qPCR analysis of representative interferon-stimulating genes (ISGs), including Cxcl10 (A) and Ifi44(B) in passage WT and *Trex1*$^{-/-}$ MEFs (n=3 biological replicates). (C) The expression of cGAS-STING pathway marker proteins in 8 passages MEFs was

analyzed by immunoblotting. (D) Quantitative analysis of p-TBK1 and p-IRF3, with GAPDH as control (n=3 biological replicates). (E-G) WT MEFs were cultured in the presence of recombinant IFN-β as indicated for 12 days. (E) The expression of p21. (F) Cells were stained for SA-β-Gal. (G) The expression levels of depicted genes were assessed by RT-qPCR (n=3 biological replicates). Data represent mean ± S.E.M. of at least 3 independent experiments. * $p < 0.05$; ** $p < 0.01$; *** $p < 0.001$, P values were calculated using one-way ANOVA versus WT with Dunnett's correction (G) For gel source data, see Mendeley Data.

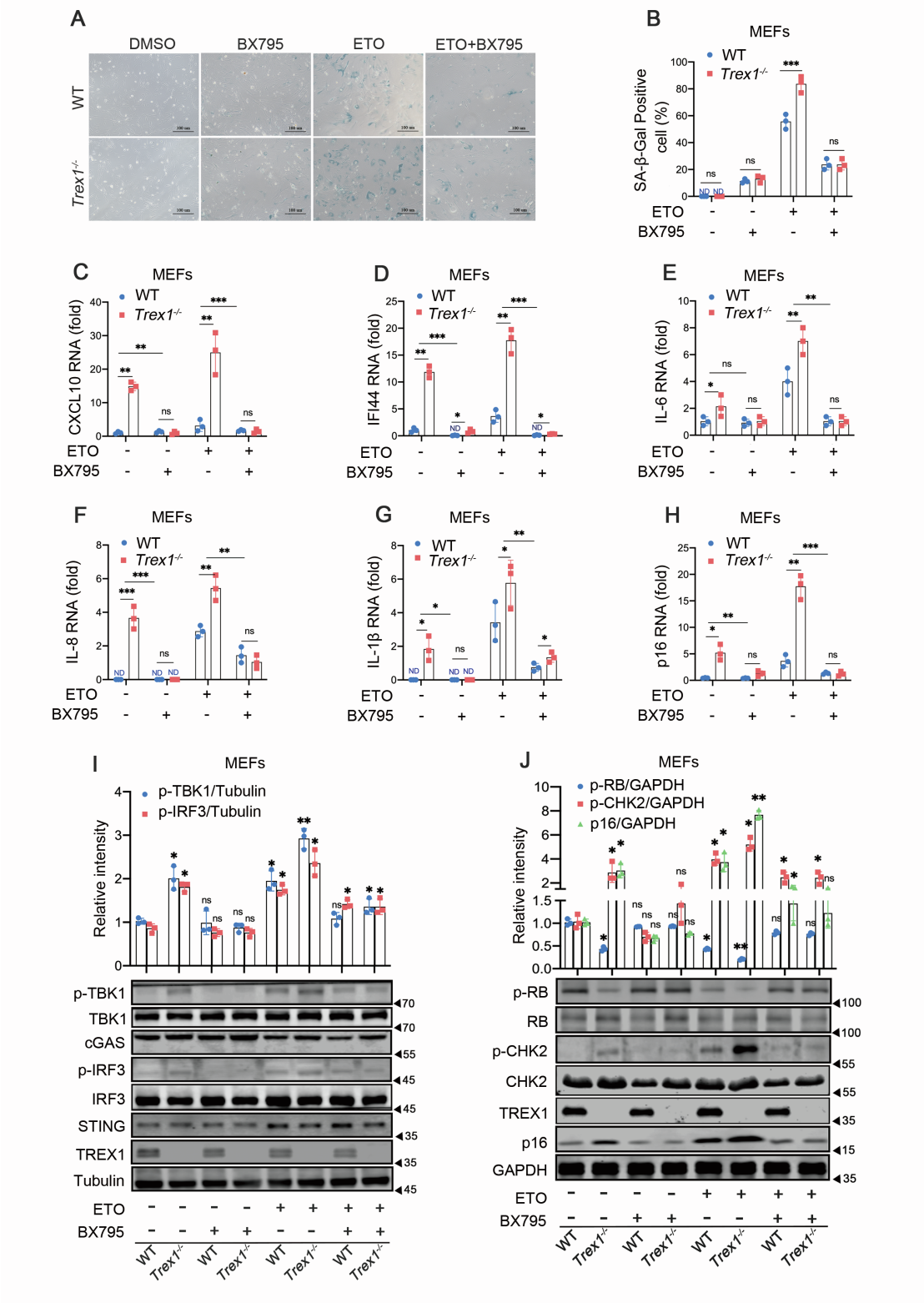

Figure S5. Inhibition of the cGAS-STING pathway alleviated cellular senescence induced by TREX1 deletion in MEFs, Related to Figure 4.

MEFs were derived from E13.5 mouse embryos. *Trex1*$^{-/-}$ MEFs were pre-treated with 10 μM ETO for 24 h, and then changed to conditioned media containing 1 μM BX795 and cultured for 5 days. (A) MEFs were subjected to SA-β-Gal analysis. (B) Histograms indicate the percentages of SA-β-Gal-positive cells (n=3 biological replicates). (C-H) Expression level of

SASP factors examined by RT-qPCR (n=3 biological replicates). (I-J) Expression of indicated proteins measured by immunoblotting (n=3 biological replicates). Data represent mean ± S.E.M. of at least 3 independent experiments. * $p < 0.05$; ** $p < 0.01$; *** $p < 0.001$, P values calculated using two-way ANOVA with Bonferroni's correction (B, C-H, J). For gel source data, see Mendeley Data.

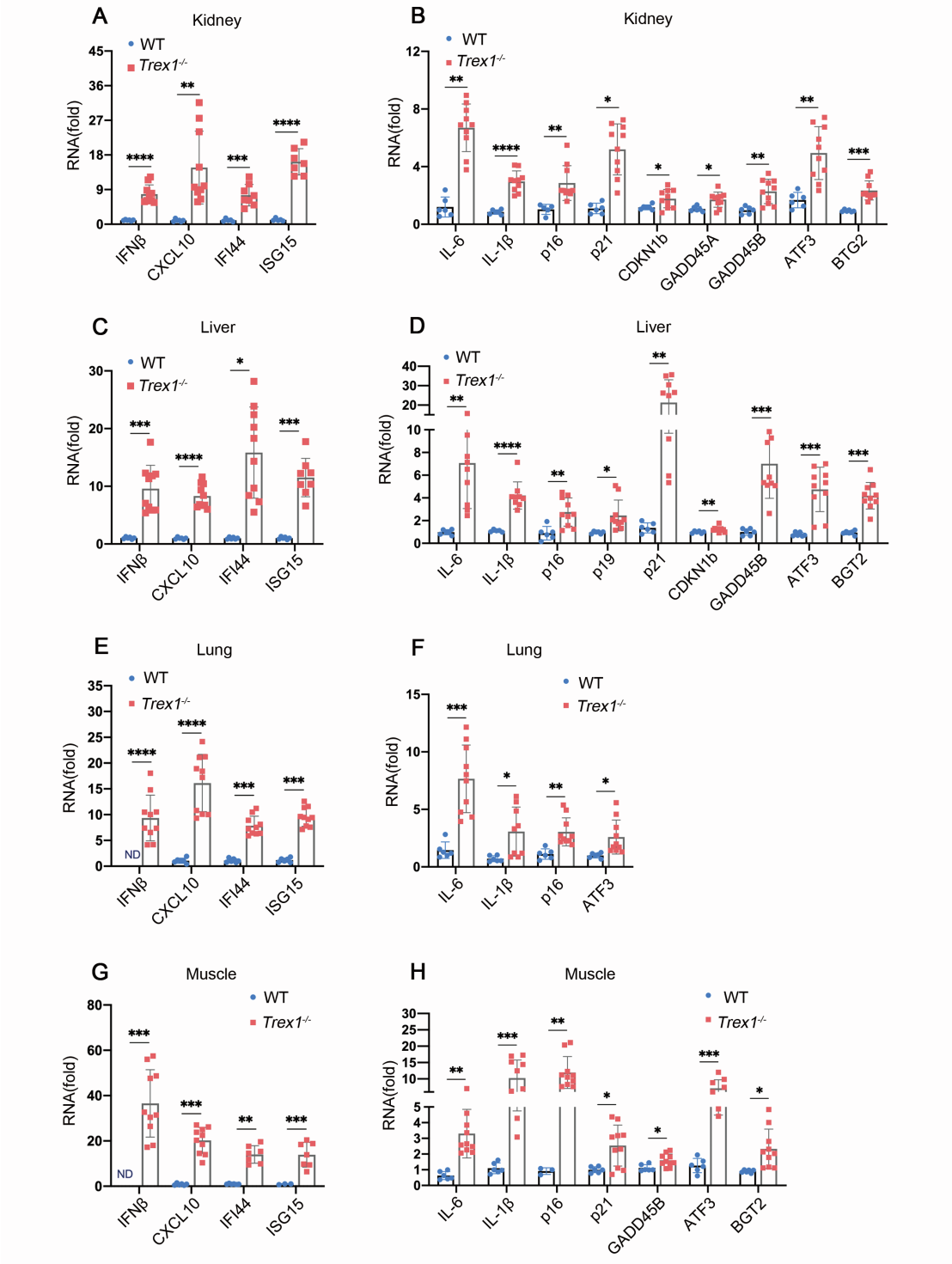

Figure S6. Cellular senescence in *Trex1* knockout lupus-like mice, Related to Figure 5. 4-5-month-old WT and *Trex1*$^{-/-}$ lupus-like mice were compared (n>6 biological replicates). (A-H) Expression level of IFNβ, ISGs, SASP factors, and aging marker proteins in kidney (A, B), liver (C, D), lung (E-F) and muscle (G, H) by RT-qPCR. Data represent mean S.E.M. of at least 3 independent experiments. * $p < 0.05$; ** $p < 0.01$; *** $p < 0.001$, P values were calculated using one-way ANOVA versus WT with Dunnett's correction (A-H).

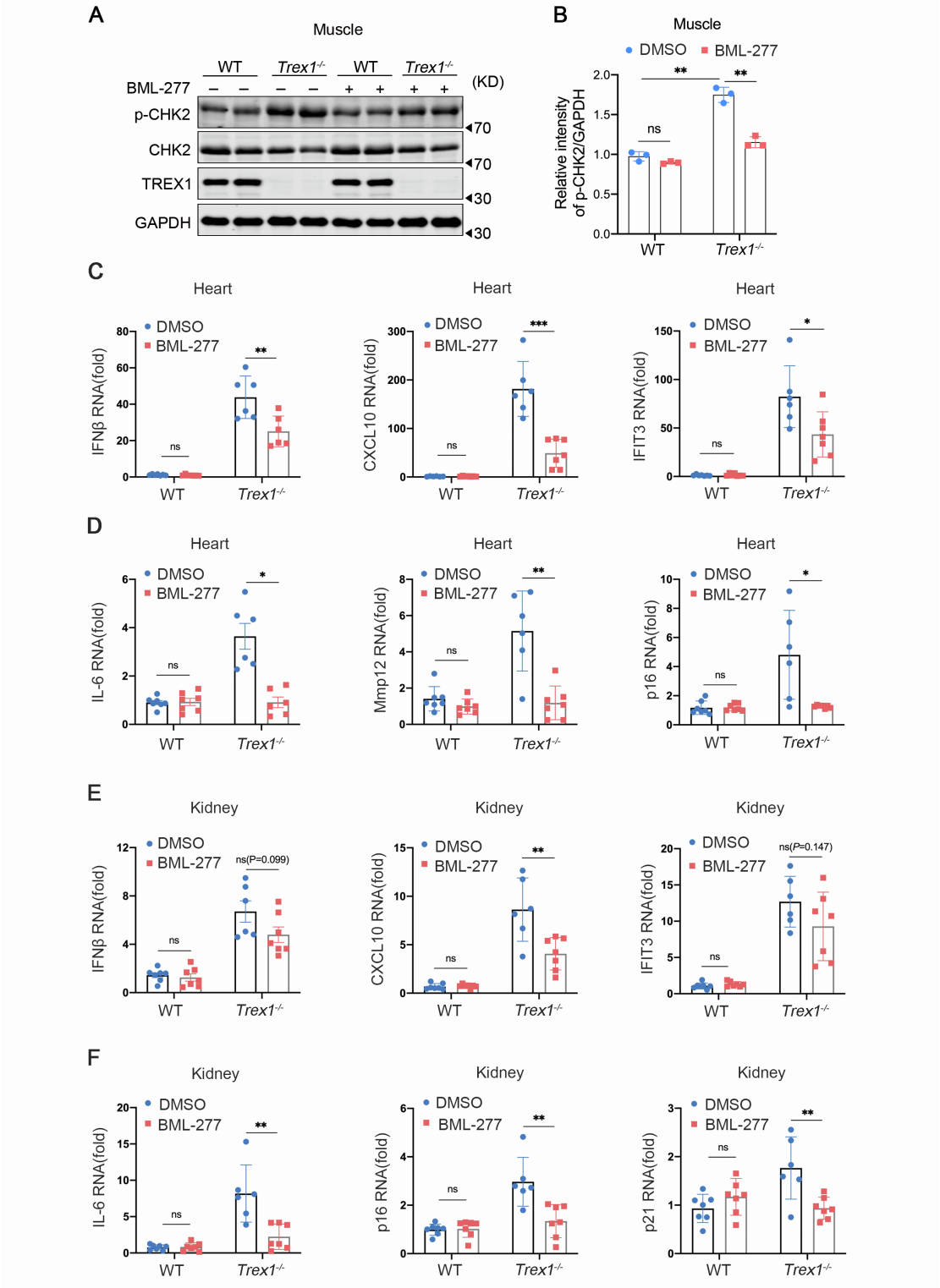

Figure S7. BML-277 alleviates lupus-like phenotypes of *Trex1*$^{-/-}$ mice, Related to Figure 6.

Trex1$^{-/-}$ mice 6 to 8 weeks of age were given a daily dose of 1 mg/kg BML-277 or solvent (5% DMSO 10% PEG300 2.5% Tween-80 in PBS) control by intraperitoneal injection for 4 weeks (n > 6 per group). (A-B) Expression of p-CHK2 in the muscle was measured by immunoblotting. (B) Quantitative analysis of p-CHK2 with GAPDH as control. ISG and SASP levels in the heart

(C-D) and kidney (E-F) were measured using RT-qPCR. Data represent mean ± S.D. or S.E.M. of at least 3 independent experiments. * $p < 0.05$; ** $p < 0.01$; *** $p < 0.001$, P values calculated using two-way ANOVA with Bonferroni's correction (B-F).

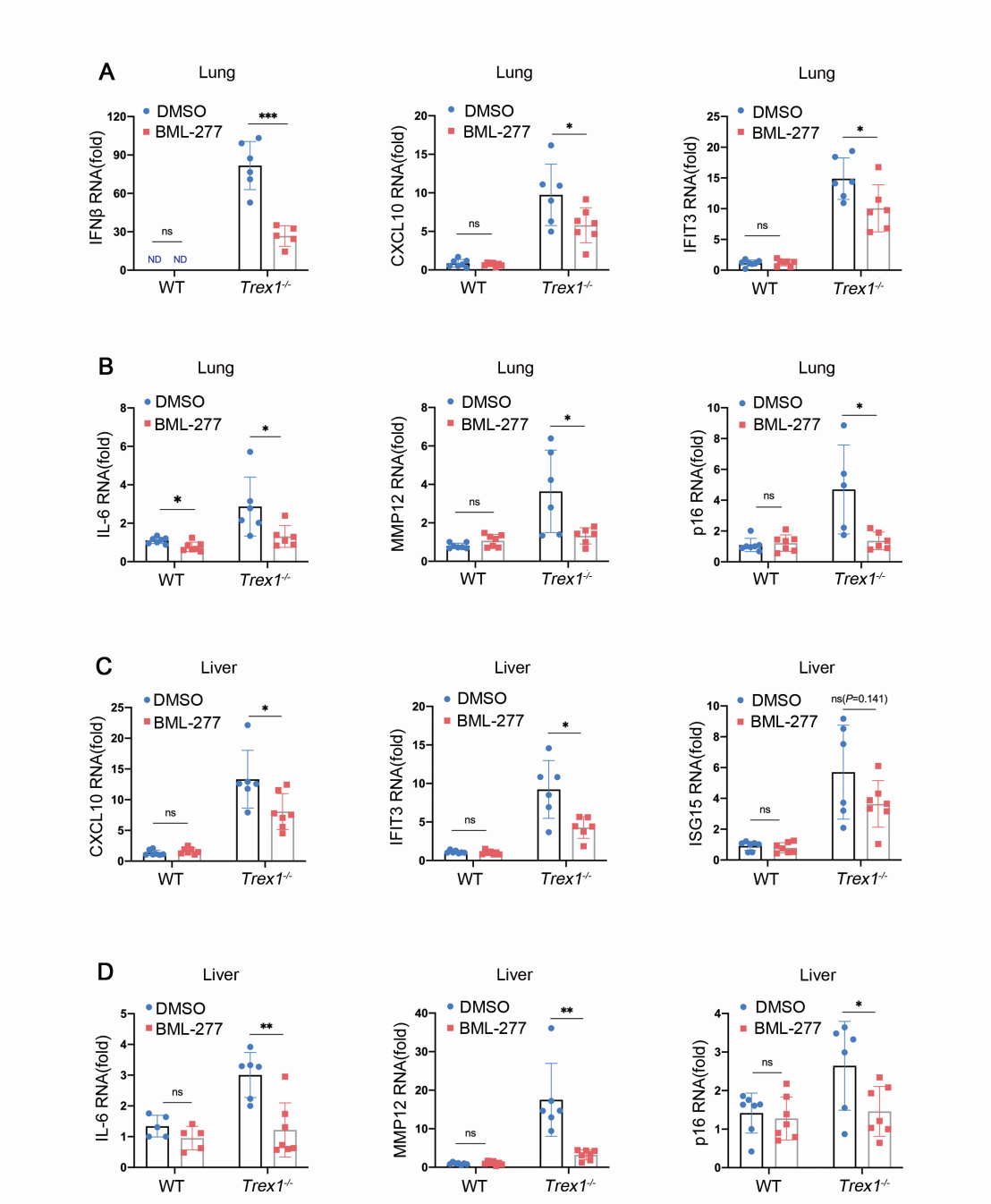

Figure S8. BML-277 alleviates lupus-like phenotypes of *Trex1*$^{-/-}$ mice, Related to Figure 6.

Trex1$^{-/-}$ mice 6 to 8 weeks of age were given a daily dose of 1 mg/kg BML-277 or solvent (5% DMSO 10% PEG300 2.5% Tween-80 in PBS) control by intraperitoneal injection for 4 weeks (n > 6 per group). ISG and SASP levels in the lung (A-B) and liver (C-D) were measured using RT-qPCR. Data represent mean ± S.D. or S.E.M. of at least 3 independent experiments. * $p < 0.05$; ** $p < 0.01$; *** $p < 0.001$, P values calculated using two-way ANOVA with Bonferroni's correction (A-D).

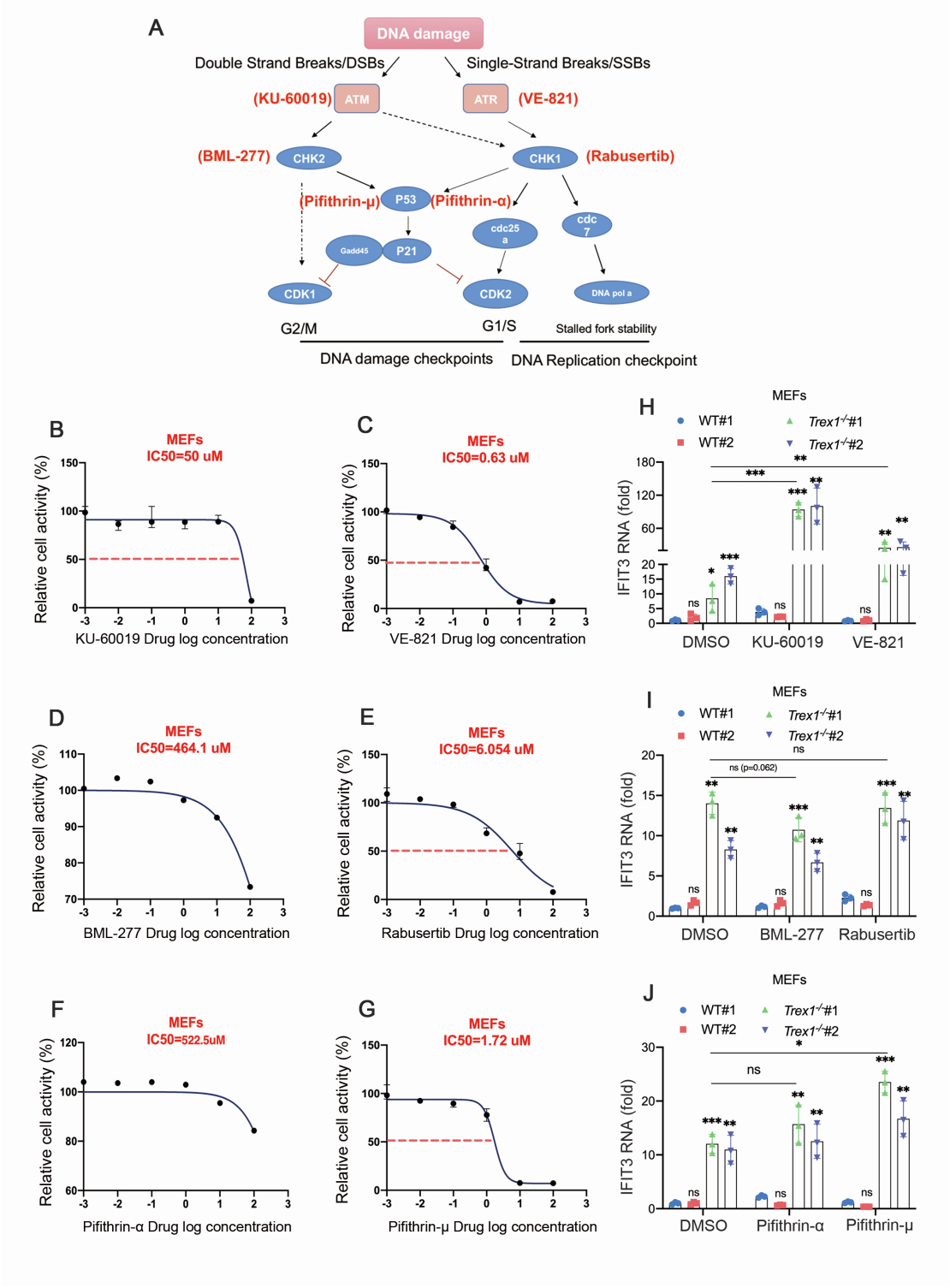

Figure S9. Screening and selection of inhibitors for DDR targets, Related to Figure 6.

(A) DNA damage response (DDR) pathway schematic showing specific candidate targets and inhibitors. (B-G) The dose responses of cell activities of selected inhibitors were tested in primary MEFs based on analysis of CCK8. The IC50 of KU-60019 (ATM), VE-821 (ATR), E (CHK1), BML-277 (CHK2), Pifithrin-α(p53) and Pifithrin-μ (p53) inhibitors were determined (n=3 biological replicates). (H-I) RT-qPCR was used to detect the effects of KU-60019 (at 10 μM ATM), VE-821 (0.1 μM ATR), Rabusertib (0.1 μM CHK1), BML-277 (1 μM CHK2), Pifithrin-μ

(0.1 μM P53), and Pifithrin-α (1 μM P53) on mRNA levels of Ifit3 in *Trex1*$^{-/-}$ MEFs (n=3 biological replicates). Data represent mean ± S.E.M. of at least 3 independent experiments. * $p < 0.05$; ** $p < 0.01$; *** $p < 0.001$, P values calculated using two-way ANOVA with Bonferroni's correction (H-J).

Supplementary Table 1. Primers used for RT-qPCR, Related to RNA isolation and real-time quantitative PCR.

Gene	Species		Primer Sequence (5′-3′)
Ifnβ	Mouse	Forward	TCCGAGCAGAGATCTTCAGGAA
		Reverse	TGCAACCACCACTCATTCTGAG
Cxcl10	Mouse	Forward	GCCGTCATTTTCTGCCTCA
		Reverse	CGTCCTTGCGAGAGGGATC
Isg15	Mouse	Forward	GGTGTCCGTGACTAACTCCAT
		Reverse	TGGAAAGGGTAAGACCGTCCT
Ifit3	Mouse	Forward	TGGCCTACATAAAGCACCTAGATGG
		Reverse	CGCAAACTTTTGGCAAACTTGTCT
Ifit44	Mouse	Forward	ATGCACAGATCTTCAAGGCCTGGGC
		Reverse	GTGCTGTGGAGTGCACAGCGGAAGT
Irf7	Mouse	Forward	ATGCACAGATCTTCAAGGCCTGGGC
		Reverse	GTGCTGTGGAGTGCACAGCGGAAGT
Oas1	Mouse	Forward	GCTGCCAGCCTTTGATGT
		Reverse	TGGCATAGATTCTGGGATCA
Il6	Mouse	Forward	GAGGATACCACTCCCAACAGACC
		Reverse	AAGTGCATCATCGTTGTTCATACA
Il8	Mouse	Forward	GTCCTTAACCTAGGCATCTTCG
		Reverse	TCTGTTGCAGTAAATGGTCTCG
Il-1β	Mouse	Forward	ACGGACCCCAAAAGATGAAG
		Reverse	TTCTCCACAGCCACAATGAG
Mmp12	Mouse	Forward	TTCATGAACAGCAACAAGGAA
		Reverse	TTGATGGCAAAGGTGGTACA
p16	Mouse	Forward	CTTCGCCGAGCAGTTTCGT
		Reverse	TCAATCCCATCAGCCATTTCC
p21	Mouse	Forward	CTGGTGATGTCCG ACCTGTT
		Reverse	TCAAAGTTCCACCGTTCTCG
p19	Mouse	Forward	CTGAACCGCTTTGGCAAGAC
		Reverse	GCCCTCTCTTATCGCCAGAT
Cdkn1b	Mouse	Forward	CCCCCAATCGCAAGGATTCTT
		Reverse	CTTGGTTCGGTGGGTCTGTC
Gadd45b	Mouse	Forward	CAACGCGGTTCAGAAGATGC
		Reverse	GGTCCACATTCATCAGTTTGGC
Gadd45a	Mouse	Forward	CCGAAAGGATGGACACGGTG
		Reverse	TTATCGGGGTCTACGTTGAGC
Atf3	Mouse	Forward	GAGGATTTTGCTAACCTGACACC
		Reverse	TTGACGGTAACTGACTCCAGC
Btg2	Mouse	Forward	ATGAGCCACGGGAAGAAC
		Reverse	GCCCTACTGAAAACCTTGAGTC
Hprt	Mouse	Forward	CAGTCCCAGCGTCGTGATTAG
		Reverse	AAACACTTTTTCCAAATCCTCGG